Formation and electric property measurement of nanosized patterns of tantalum oxide by current sensing atomic force microscope

Young-ho Kim, Jianwei Zhao, and Kohei Uosaki[a)]
Physical Chemistry Laboratory, Division of Chemistry, Graduate School of Science, Hokkaido University, Sapporo 060-0810, Japan

(Received 25 August 2003; accepted 29 September 2003)

Nanosized patterns of tantalum oxide were fabricated on a tantalum substrate by applying a potential pulse utilizing current sensing atomic force microscopy (CSAFM). The dimensions of the dots were strongly dependent on the bias applied, scan rate, and potential pulse duration. By controlling these variables, the minimum size nanodots with full width at half maximum of 35 nm was achieved. Immediately after pattern formation, the electrical properties of the Ta oxide nanodots were measured using CSAFM. The charge transport at the CSAFM tip and the nanosized Ta oxide dot can be described by Poole–Frenkel type conduction. The relative dielectric constant of the nanosized Ta_2O_5 dots was calculated to be 17.8–24.3, showing that the quality of the oxide was high. In addition, by controlling the substrate bias applied, pulse duration, and tip scan speed, nanosized Ta oxide lines with the desired dimensions were prepared. © *2003 American Institute of Physics.* [DOI: 10.1063/1.1627951]

I. INTRODUCTION

Recently, nanotechnologies have attracted the attention of many research groups. One of the most important targets of nanotechnology research is the construction of nanosized electronic devices. To achieve this goal, advances in nanometer scale manipulation of metal or semiconductor surfaces is essential. It is difficult to modify metal or semiconductor surfaces on a nanometer scale by optical or electron beam lithography but scanning probe lithography (SPL) is considered to be a promising tool for solving this difficulty.[1,2]

There are two major SPM-based lithography techniques. One is based on a mechanical mechanism that uses an atomic force microscope (AFM)[3–8] and the other is based on an electrical mechanism that uses a scanning tunneling microscope (STM).[9–16] A current sensing atomic force microscope (CSAFM)-based SPL has been demonstrated to be a useful method for utilizing the advantages of both STM and AFM. We used CSAFM to form a nanosized pattern of a self-assembled monolayer on a gold substrate.[17,18] CSAFM has also been used to create nanosized surface oxide structures on metal and semiconductor surfaces.[19–29] Many kinds of metal oxides, such as TiO_2,[20,24–26] Al_2O_3,[21,27] and Cr oxides[28] were fabricated using CSAFM. It is generally believed that oxide is formed as a result of anodic oxidation with the tip and the ambient moisture layer between the tip and the substrate acting as a nanosized counter electrode and an electrolyte solution, respectively, as schematically shown in Fig. 1.[29]

Tantalum pentoxide is one of the best candidates for a high performance dielectric material to be used in various modern electronic devices[30–35] because of its superior electronic properties such as high dielectric constant [amorphous: 29.2–29.5 (Ref. 30) and crystalline: 45.6–51.7 (Ref. 30)], low dielectric loss and low leakage current as well as having good chemical and thermal stabilities. To apply tantalum oxide for fabrication of metal–insulator–metal (MIM) or metal–oxide–semiconductor (MOS) junction-based nanoelectronic devices, control of the oxide dimensions and electrical reliability on a nanometer scale is required.

In this study, we report the construction of tantalum anodic oxide nanopatterns on a sputtered tantalum film by applying the bias in air using the CSAFM in contact mode. Immediately after the formation of the nanosized pattern, the current (I)–voltage (V) relationship of the nanosize tantalum oxide was also measured using the CSAFM. Reproducible $I-V$ curves were obtained at an extremely high electric field ($>$0.1 MV/m), suggesting high breakdown voltage of the nanosized tantalum oxide patterns. Our $I-V$ results are explained by means of the Poole–Frenkel conduction mechanism in a comparison with theoretical simulation.[36–40]

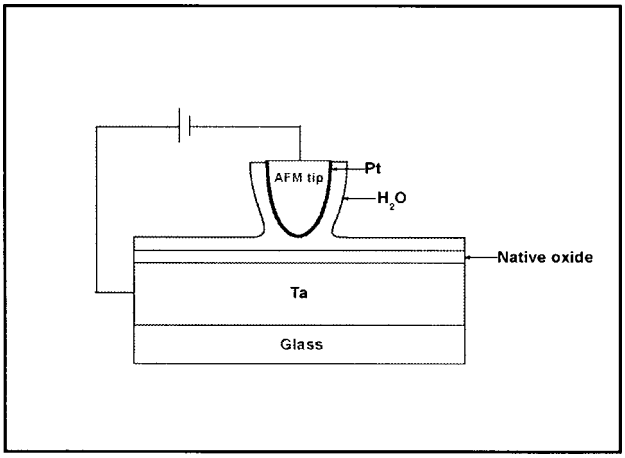

FIG. 1. Schematic of oxide formation on water covered Ta with native oxide using CSAFM.

a)Author to whom correspondence should be addressed; electronic mail: uosaki@pcl.sci.hokudai.ac.jp

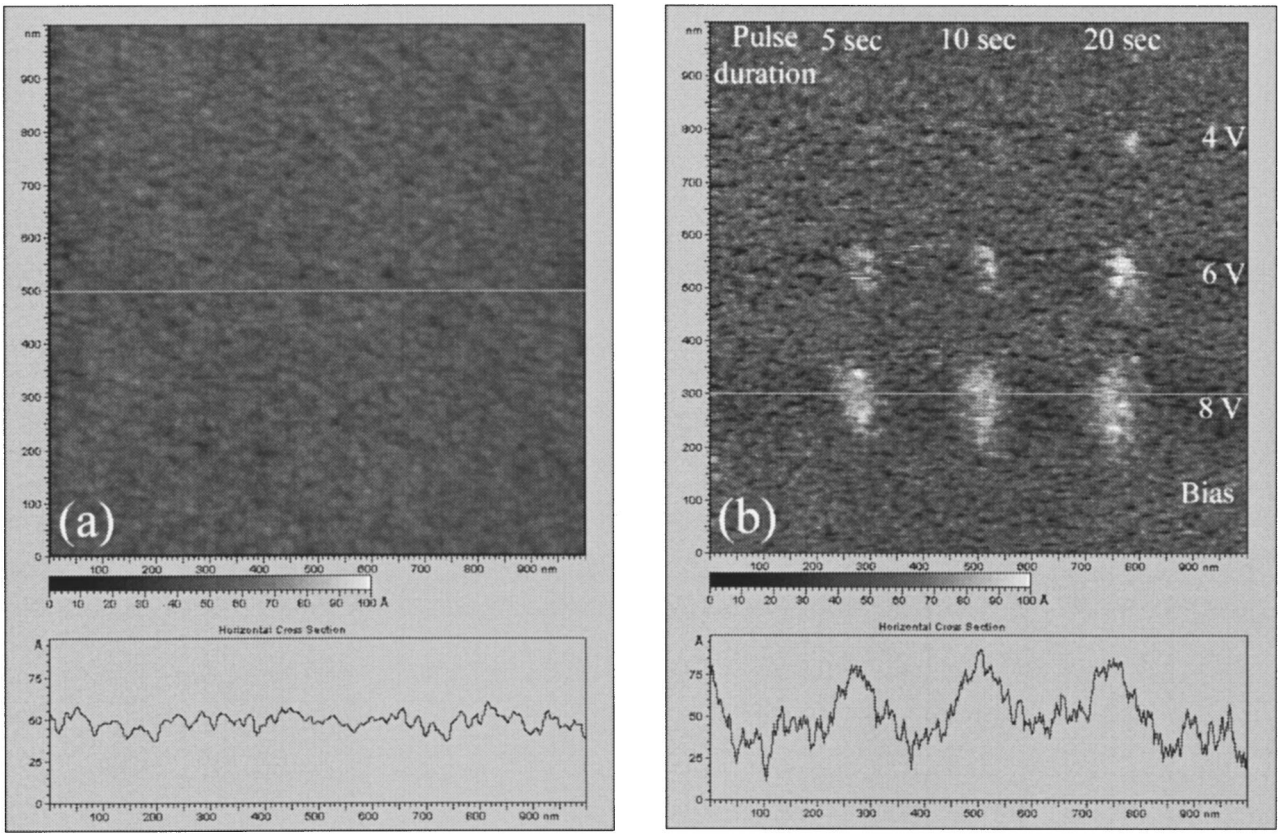

FIG. 2. (a) AFM image ($1\ \mu m \times 1\ \mu m$) of the sputtered tantalum film covered (top panel) with native oxide and cross-sectional profile (bottom panel). (b) AFM image of oxide dots fabricated by applying various substrate biases of 4, 6, and 8 V and various pulse duration times of 5, 10, 20 s. The bottom panel shows the cross-sectional profile of the dots generated by 8 V pulses.

II. EXPERIMENT

Tantalum films (thickness: ~160 nm) were sputtered on a nonalkaline glass sheet. A native oxide layer formed as the sputtered tantalum film was exposed to air. The thickness of the native oxide layer was ~2 nm measured by spectroscopic ellipsometry (GESP-5, SOPRA) using a 30 W Xe lamp as the light source. This value is in good agreement with previously reported values (~2–3 nm).[41–43]

CSAFM measurements were carried out using a PicoSPM microscope (Molecular Imaging) and a PicoScan controller (Molecular Imaging). Pattern formation was achieved by applying bias between the Pt coated conductive Pt/Si_3N_4 tip (MikroMasch, typical spring constant: 0.12 N/m, parabolic shape with an apex of the radius of curvature: <35 nm) and the Ta substrate at room temperature (~23 °C) and ambient humidity of $\sim 38 \pm 2\%$. The $I-V$ curves of the nanosized dot patterns were also measured in air using the CSAFM setup.

III. RESULTS AND DISCUSSION

Figure 2(a) is an AFM image of the initial surface covered with a native oxide with grains of ~20 nm diameter. Potential pulses of various biases and duration times were applied at various locations of the surface without tip scanning. Figure 2(b) shows AFM images of the surface after bias of 4, 6, and 8 V (the substrate is positive) for durations of 5, 10, and 20 s. From the cross-sectional profiles of the patterns formed at 8 V, shown in the bottom panel of Fig. 2(b), it seems that the dot pattern has a conical shape. However, it should also be noted that it is possible that the virtual image due to the tip is shaped like an inverted triangle. Therefore, we estimate that the erupted nanosize Ta oxide

TABLE I. Effect of substrate bias (4, 6, and 8V) and pulse duration on the dimensions of nanosized dots.

Pulse duration (s)	4V		6V		8V	
	Height (nm)	FWHM (nm)	Height (nm)	FWHM (nm)	Height (nm)	FWHM (nm)
5	···	···	4.5	30	5.0	70
10	···	···	5.5	35	6.5	50
20	4.0	35	6.5	50	8.0	80

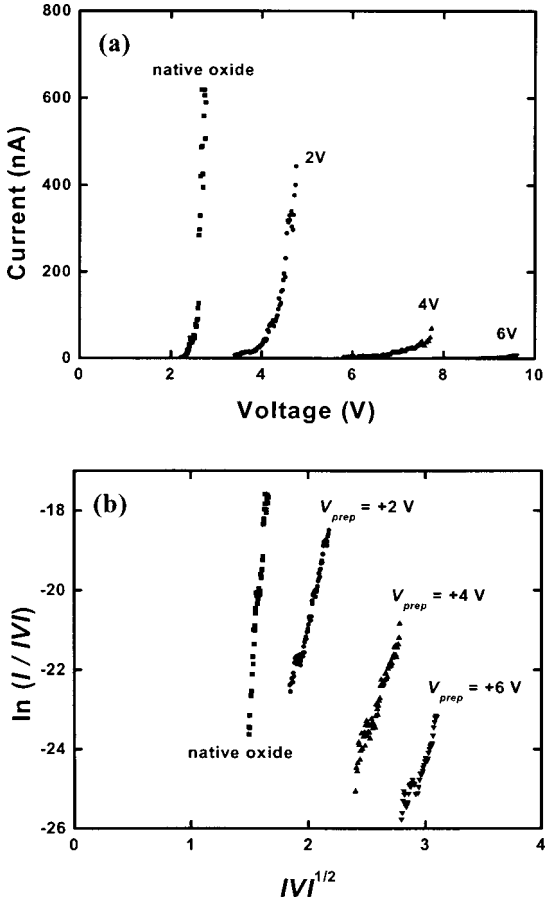

FIG. 3. (a) $I-V$ curves of the nanodots fabricated by substrate bias of 2, 4, and 6 V obtained using the CSAFM tip. The result for the Ta substrate with native oxide is also shown for comparison. (b) Poole–Frenkel, $\ln(I/V)$ vs $V^{1/2}$, plots of (a).

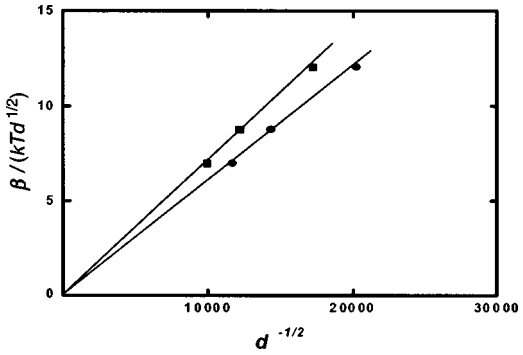

FIG. 4. Relationship between the slope of $\ln(I/V)$ and $V^{1/2}$ plots [Fig. 3(b)], i.e., $\beta/(kTd^{1/2})$, and $d^{-1/2}$ which was estimated using both cylindrical (square) and conical (circle) Ta oxide dots.

dot pattern is shaped somewhere between conical and cylindrical. The size of the dot strongly depended on both the amplitude and duration of the potential pulse, a summary of which is in Table I.

In the case of 4 V substrate bias, no clear patterns were observed if the pulse duration was 5 or 10 s, but a distinguishable feature with height of ~4 nm and full width at half maximum (FWHM) of ~35 nm was observed upon application of a 20 s pulse. With the 6 and 8 V bias, dots formed even for a 5 s pulse. It has been reported that the main factors controlling the pattern size are the ambient humidity level, scanning speed, pulse duration, bias applied, and tip radius.[25,26] Furthermore, the dimension of the dot is strongly dependent on the initial roughness of the metal substrate and drift of the tip during the patterning process, which results in pattern broadening.

Observation of the nanosized dot after the potential pulse suggests the formation of tantalum oxide because the density of Ta is much higher than that of Ta_2O_5 and, therefore, the oxidation process results in a volume increase. The density of Ta metal is 16.65 g/cm^3 and the theoretical density of crystalline Ta_2O_5 (hexagonal) is ~8.3 g/cm^3.[44] The density of amorphous Ta_2O_5 varies over a considerable range depending on the fabrication conditions.[44] Based on these density values, the volume of crystalline Ta_2O_5 is ~2.45 times that of Ta metal for the same number of Ta atoms. To calculate the total thickness of the oxide, we used both a conical shape as observed by AFM and a cylindrical shape for the Ta oxide dot because of the reason mentioned above. Ta oxide below the initial plane is considered to be cylindrical in both cases. For the Ta oxide with a conical shape, the erupted height of the Ta oxide was ~81% of the entire Ta oxide thickness and the calculated total thicknesses of the Ta oxide layers were 4.9, 8.0, and 9.8 nm for bias of 4, 6, and 8 V, respectively. The total thickness of the Ta oxide is proportional to the bias applied with a slope of 1.23 nm/V. On the other hand, if a cylindrical shape is assumed, the total calculated thicknesses of the Ta oxide layers were 6.8, 11.0, and 13.5 nm for bias of 4, 6, and 8 V, respectively. In this case, the oxide growth rate was 1.69 nm/V and the height ratio (the erupted height of the Ta oxide dot pattern/the thickness of the whole oxide layer) was 59%.

It is well known that there is a linear relationship between the anodization voltage and the oxide thickness in the case of anodic oxide growth.[45] It is quite interesting that the growth rate of the present nanosized Ta oxide dot pattern (~1.23–1.69 nm/V) is comparable to the growth rate of the tantalum anodic oxide (~1.7 nm/V).[46,47] Thus, it is reasonable to consider that the growth mechanism for the nanosized oxide is electrochemical anodic oxidation as schematically shown in Fig. 1.

To examine the quality of the nanosized Ta oxide dot pattern, the local electrical property was investigated using CSAFM immediately after nanosize dot formation. Because of possible application of dielectric Ta oxide for a microelectronic device, the $I-V$ relationship is one of the crucial characteristics. The $I-V$ relationship was measured at room temperature by applying only a cathodic substrate bias. We did not apply an anodic substrate bias in order to avoid further growth of the Ta oxide. The Pt-coated tip/Ta oxide/Ta substrate structure is considered to be a MIM junction.

Figure 3(a) shows the $I-V$ curves of the Ta anodic oxide nanosized dots prepared by applying 2, 4, and 6 V bias. As a comparison, the $I-V$ curve of Ta with native oxide is also shown. As preparation bias increased, the onset potential of the current flow increased. Since the available maximum bias of the present CSAFM setup was 10 V, the $I-V$ curves of the

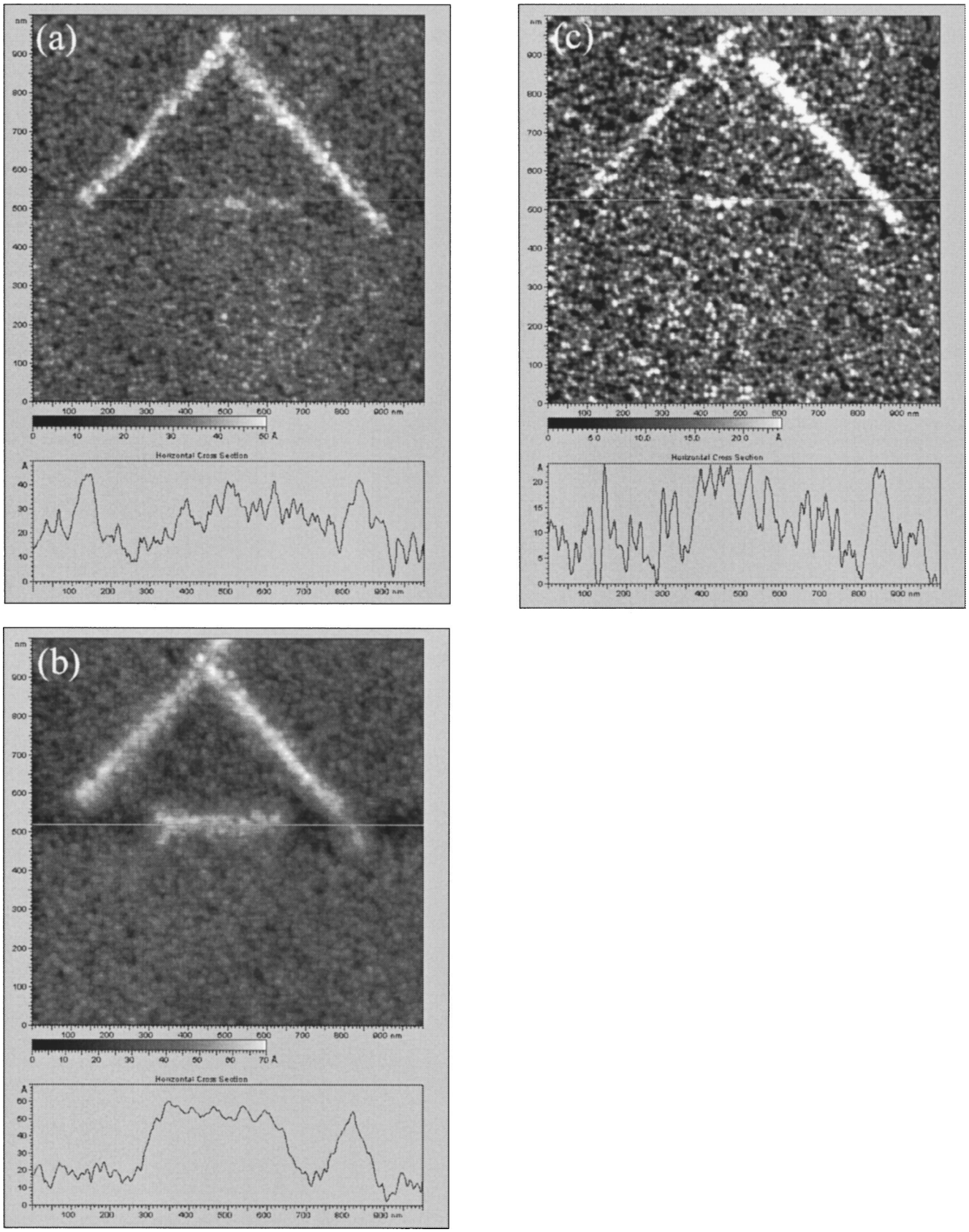

FIG. 5. AFM images of line patterns fabricated by applying various substrate bias and scanning rates. Cross-sectional profiles at the lines shown in the AFM images are given in the bottom panels. (a) Substrate bias of 6 V and scanning rate of 50 nm/s; (b) substrate bias of 8 V and scanning rate of 50 nm/s; (c) substrate bias of 6 V and scanning rate of 500 nm/s.

Ta oxide dots prepared with more than 6 V bias could not be obtained.

Tantalum oxide grown on a Ta substrate is normally nonstoichiometric and contains many defects. These defects can behave as coulombic traps. According to the Poole–Frenkel mechanism, the energy barrier of the coulombic trap becomes asymmetric in an electric field and results in the thermal ionization of trapped charge carriers.[37,38] Thus, the $I-V$ relationship of the tantalum oxide film in a high electric field is described by Poole–Frenkel type conduction as[48–54]

$$\ln\left(\frac{I}{V}\right)=\frac{\beta}{kTd^{1/2}}\sqrt{V}+\left(\ln C-\frac{e\Phi}{kT}\right), \tag{1}$$

where β is the field-lowering coefficient and is given by

$$\beta=\left(\frac{e^3}{\pi\varepsilon\varepsilon_0}\right)^{1/2}, \tag{2}$$

where k is the Boltzmann constant, T is the absolute temperature, C is the proportionality constant, e is the elementary charge, Φ is the ionization potential, ε_0 is the permittivity of free surface, ε is the relative dielectric constant, and d is the film thickness. According to the Poole–Frenkel relation given in Eq. (1), a linear relationship is expected between $\ln(I/V)$ and $V^{1/2}$ with slope of $\beta/(kTd^{1/2})$, which is a function of the relative dielectric constant and the thickness of the material at a given temperature. Poole–Frenkel plots using the results shown in Fig. 3(a) are shown in Fig. 3(b). In all the cases, very good linear relationships were obtained, confirming the Poole–Frenkel conduction mechanism.

Figure 4 shows the relationship between the slope of the $\ln(I/V)$ and $V^{1/2}$ plots [Fig. 3(b)], i.e., $\beta/(kTd^{1/2})$ and $d^{-1/2}$, which were estimated using both the cylindrical and conical Ta oxide dots described above. Very good linear relationships, which pass through the origin, were obtained in both cases. From the slopes, the field-lowering coefficient, β, is determined to be $1.54-1.86\times10^{-5}$ eV $m^{1/2}/V^{1/2}$. One can obtain the relative dielectric constants using these values as 17.8–24.3. The relative dielectric constant of Ta_2O_5 film is reported to be dependent on the thickness but is 18.5 for thin anodic oxide films of less than 19 nm.[46] The experimentally observed value is in good agreement with this value, confirming the nanosized dots prepared in this study have dielectric properties similar to Ta_2O_5.

With application of nanoelectronic devices in mind, line pattern formation was attempted on the native oxide covered Ta substrate using CSAFM by scanning the position of the conductive AFM tip. No clear feature was observed when 4 V bias was applied. This must be because the scan rate of the tip was too fast at 4 V bias. The formation of the nanosized dot with a stationary tip at 4 V bias required a relatively long pulse duration (>20 s) as already shown [Fig. 2(b)] but the slowest tip scan rate of the present CSAFM system is 50 nm/s. Clear line patterns can be formed using 6 and 8 V bias with the tip scan rate 50 nm/s as shown in Figs. 5(a) and 5(b), respectively. The height and the FWHM of the patterned lines formed by substrate bias of 6 V are ~4.2 and ~70 nm, respectively, and those with substrate bias of 8 V are ~3.4 and ~100 nm, respectively. The FWHMs of the lines are bigger than those of the dots maybe because of drift of the tip during the scanning process. The smallest line dimension in this study (height: ~1.9 nm, FWHM: ~50 nm) was achieved at substrate bias of 6 V with a scanning rate of 500 nm/s as shown in Fig. 5(c). The height of the pattern is close to the roughness of the substrate so one needs to use a much flatter surface to create a pattern of smaller dimensions.

IV. CONCLUSIONS

In summary, we have demonstrated that nanosized tantalum oxide dots can be prepared on a Ta substrate with native oxide by applying the potential pulse using CSAFM (the substrate is positive to the tip) in air. The FWHM of the smallest dots was 35 nm. The $I-V$ characteristics of the nanosized tantalum oxide dots were measured immediately after dot formation also using CSAFM. These results showed that the nanosized Ta oxide dots essentially grew as a result of the electrochemical anodic oxidation mechanism and charge transport at the CSAFM tip and that the nanosized Ta oxide dot can be described by Poole–Frenkel type conduction. The relative dielectric constant of the nanosized Ta_2O_5 dots was calculated to be 17.8–24.3, showing that the quality of the oxide was high. In addition, by controlling the substrate bias applied, pulse duration and tip scan speed, nanosized Ta oxide lines with the desired dimensions were prepared. To obtain a pattern with smaller dimensions, drift of the tip and the initial surface roughness should be minimized.

ACKNOWLEDGMENT

The authors thank Professor W. K. Paik for help with the spectroscopic ellipsometry measurements.

[1] R. W. Carpick and M. Salmeron, Chem. Rev. (Washington, D.C.) **97**, 1163 (1997).
[2] R. M. Nyffenegger and R. M. Penner, Chem. Rev. (Washington, D.C.) **97**, 1195 (1997).
[3] H. T. Lee, S. J. Park, K. H. Park, J. S. Ha, H. J. Yoo, and J. Y. Koo, J. Vac. Sci. Technol. A **15**, 1451 (1997).
[4] M. Koinuma and K. Uosaki, J. Vac. Sci. Technol. B **12**, 1543 (1994).
[5] M. Koinuma and K. Uosaki, Electrochim. Acta **40**, 1345 (1995).
[6] G. Y. Liu, S. Xu, and Y. Qian, Acc. Chem. Res. **33**, 457 (2000).
[7] S. Xu, P. E. Laibinis, and G. Y. Liu, J. Am. Chem. Soc. **120**, 9356 (1998).
[8] N. A. Amro, S. Xu, and G. Y. Liu, Langmuir **16**, 3006 (2000).
[9] J. K. Schoer, F. P. Zamborini, and R. M. Crooks, J. Phys. Chem. **100**, 11086 (1996).
[10] C. B. Gorman, R. L. Carroll, Y. He, F. Tian, and R. Fuierer, Langmuir **16**, 6312 (2000).
[11] Y. T. Kim and A. J. Bard, Langmuir **8**, 1096 (1992).
[12] J. K. Schoer and R. M. Crooks, Langmuir **13**, 2323 (1997).
[13] J. Chen, M. A. Reed, C. L. Asplund, A. M. Cassell, M. L. Myrick, A. M. Rawlett, J. M. Tour, and P. G. Van Patten, Appl. Phys. Lett. **75**, 624 (1999).
[14] W. Mizutani, T. Ishida, and H. Tokumoto, Langmuir **14**, 7197 (1998).
[15] U. Gratratzke and G. Simon, Phys. Rev. B **52**, 8535 (1995).
[16] J. Hartwich, M. Sundermann, U. Kleineberg, and U. Heinzmann, Appl. Surf. Sci. **144–145**, 538 (1999).
[17] J. W. Zhao and K. Uosaki, Nano Lett. **2**, 137 (2002).
[18] J. W. Zhao and K. Uosaki, Langmuir **17**, 7784 (2001).
[19] E. S. Snow and P. M. Campbell, Science **270**, 1639 (1995).
[20] E. S. Snow and P. M. Campbell, Physica B **227**, 279 (1996).
[21] A. Olbrich, B. Ebersberger, C. Boit, J. Vancea, H. Hoffmann, H. Altmann, G. Gieres, and J. Wecker, Appl. Phys. Lett. **78**, 2934 (2001).
[22] M. Tello and R. Garcia, Appl. Phys. Lett. **79**, 424 (2001).

[23] M. Lazzarino, S. Heun, B. Ressel, and K. C. Prince, Appl. Phys. Lett. **81**, 2842 (2002).
[24] K. Kobayashi, Y. Tomita, and S. Yoshida, Nano Lett. **2**, 925 (2002).
[25] R. Held, T. Heinzel, P. Studerus, and K. Ensslin, Physica E (Amsterdam) **2**, 748 (1998).
[26] C. Huh and S. J. Park, J. Vac. Sci. Technol. B **18**, 55 (2000).
[27] E. S. Snow, D. Park, and P. M. Campbell, Appl. Phys. Lett. **69**, 269 (1996).
[28] D. Wang, L. Tsau, and K. L. Wang, Appl. Phys. Lett. **67**, 1295 (1995).
[29] H. Sugimura and N. Nakagiri, Jpn. J. Appl. Phys., Part 1 **34**, 3406 (1995).
[30] P. C. Joshi and M. W. Cole, J. Appl. Phys. **86**, 871 (1999).
[31] Y. Nakagawa and T. Okada, J. Appl. Phys. **68**, 556 (1990).
[32] S. Tanimoto, M. Matsui, K. Kamisako, K. Kuroiwa, and Y. Tarui, J. Electrochem. Soc. **139**, 320 (1992).
[33] Y. Nishimura, K. Tokunaga, and M. Tsuji, Thin Solid Films **226**, 144 (1993).
[34] K. W. Kwon, C. S. Kang, S. O. Park, H. K. Kang, and S. T. Ann, IEEE Trans. Electron Devices **43**, 919 (1996).
[35] J. Y. Zhang, B. Lim, V. Dusastre, and I. W. Boyd, Appl. Phys. Lett. **73**, 2299 (1998).
[36] J. Frenkel, Phys. Rev. **54**, 647 (1938).
[37] W. R. Harrell and J. Frey, Thin Solid Films **352**, 195 (1999).
[38] W. R. Harrell and C. Gopalakrishnan, Thin Solid Films **405**, 205 (2002).
[39] V. I. Kol'dyaev, Philos. Mag. B **79**, 331 (1999).
[40] S. D. Ganichev, E. Ziemann, and W. Prettl, Phys. Rev. B **61**, 10361 (2001).
[41] D. J. Smith and L. Young, Thin Solid Films **101**, 11 (1983).
[42] V. A. Macagno and J. W. Schultze, J. Electroanal. Chem. **180**, 157 (1984).
[43] H. J. Mathieu and D. Landolt, Surf. Interface Anal. **5**, 77 (1983).
[44] C. Chaneliere, J. L. Autran, R. A. B. Devine, and B. Balland, Mater. Sci. Eng., R. **22**, 269 (1998).
[45] C. J. Dell'Oca, D. J. Pulfrey, and L. Young, in *Physics of Thin Films*, edited by M. H. Francomb and R. W. Hoffmann (Academic, London, 1971), Vol. 6.
[46] O. Kerrec, D. Devilliers, H. Groult, and M. Chemla, Electrochim. Acta **40**, 719 (1995).
[47] I. Montero, J. M. Albella, and J. M. Martinez-Duart, Electrochim. Acta **35**, 855 (1990).
[48] Y. S. Kim, Y. H. Lee, K. M. Lim, and M. Y. Sung, Appl. Phys. Lett. **74**, 2800 (1999).
[49] C. Chaneliere, S. Four, J. L. Autran, and R. A. B. Devine, Microelectron. Reliab. **39**, 261 (1999).
[50] C. Chaneliere, J. L. Autran, and R. A. B. Devine, J. Appl. Phys. **86**, 480 (1999).
[51] M. Houssa, R. Degraeve, P. W. Mertens, M. M. Heyns, J. S. Jeon, A. Halliyal, and B. Ogle, J. Appl. Phys. **86**, 6462 (1999).
[52] S. Blonkowski, M. Regache, and A. Halimaoui, J. Appl. Phys. **90**, 1501 (2001).
[53] S. Ezhilvalavan and T. Y. Tseng, J. Appl. Phys. **83**, 4797 (1998).
[54] A. Paskaleva, E. Atanassova, and T. Dimitrova, Vacuum **58**, 470 (2000).